

POWER DISTURBANCE IDENTIFICATION BASED ON TRANSIENT BEHAVIORS USING MORPHOLOGICAL MAX-LIFTING SCHEME AND NONLINEAR PRINCIPAL COMPONENT ANALYSIS

Y. Zhang[◇]
zhangyin0830@126.com

T. Y. Ji[◇]
tyji@scut.edu.cn

M. S. Li[◇]
mengshili@scut.edu.cn

Q. H. Wu^{◇ †}
wuqh@scut.edu.cn

[◇] School of Electrical Power Engineering, South China University of Technology (SCUT), Guangzhou, 510640, China.

[†] Department of Electrical Engineering and Electronics, The University of Liverpool, Liverpool L69 3GJ, U.K.
 Corresponding author: Dr T. Y. Ji; Email: tyji@scut.edu.cn

ABSTRACT

When a power system is contaminated by power quality problems, a short transition will appear before power system restoring to a new stability state. The short transitions of various power disturbances correspond to different principal component characteristics. According to these characteristics, in this paper, a scheme based on transient behaviors using morphological max-lifting scheme (MMLS) and nonlinear principal component analysis (NLPCA) is developed for the identification of power disturbances. PSCAD/EMTDC is applied to simulate six types of power disturbances, and massive simulation work has been conducted to demonstrate the effectiveness and feasibility of the proposed scheme.

INTRODUCTION

In the past few years, power disturbances have become an important issue in industrial and academic fields due to the serious power and economic loss caused by them [1]. To limit the negative effects of power disturbances on power systems, it is necessary to identify these power disturbances quickly and accurately. Nowadays, identification of power disturbances mainly adopts methods based on signal processing, fuzzy logic [2], neural network or genetic algorithm [3]. In this paper, morphological max-lifting scheme (MMLS) is employed to detect the existence of power disturbances, and nonlinear principal component analysis (NLPCA) is used for extracting the nonlinear principal components of the two-dimension signals converted from the power quality signal, which are then used to classify the power disturbance.

MM, a nonlinear analysis method based on signal processing in time domain, is excellent in noise removal and fast calculation [4]. MM is mainly applied to extract specific features in the neighborhood of every sample in the signal under analysis [5]. Two basic operators of MM are erosion (ε) and dilation (δ). Let f and g denote the signal under analysis and structuring element (SE), respectively. Erosion and dilation can be defined as follows respectively [6]:

$$\varepsilon_g(f) = f \ominus g = \bigcup_{x \in g} (f + g) \quad (1)$$

$$\delta_g(f) = f \oplus g = \bigcap_{x \in g} (f - g). \quad (2)$$

Erosion and dilation are operators that allow to eliminate or to remark special components of the signal under analysis. Opening is a morphological operator that performs dilation on the signal eroded by the same SE [7], that is, $f \circ g = (f \ominus g) \oplus g$, where \circ denotes the opening operator. Closing is a morphological operator that performs erosion on the signal dilated by the same SE [7], that is, $f \bullet g = (f \oplus g) \ominus g$, where \bullet denotes the closing operator.

The lifting scheme or simply lifting is a simple but quite powerful tool to extract some special features of the signal under analysis [8]. As a popular lifting scheme, the max-lifting scheme can preserve local maximum values of the signal being processed with high calculation speed [9].

NLPCA is commonly seen as a nonlinear generalization of principal component analysis (PCA) [10]. It can extract the linear and nonlinear principal components of the signal being processed. NLPCA can be realized by using a neural network with an auto-associative architecture [11]. Compared with other nonlinear analysis methods, such as locally linear embedding (LLE), Isomap, principal curves and self-organizing maps (SOM), NLPCA can be applied to incomplete data sets by modeling only the second part of the auto-associative network, the reconstruction or generation part [12].

In this paper, a power disturbance identification scheme based on transient behaviors using MMLS and NLPCA is proposed. The proposed scheme only needs process a data window of one and a half cycles, which remarkably reduces calculation burden.

POWER QUALITY DISTURBANCE IDENTIFICATION SCHEME

The power quality disturbance identification scheme proposed in this paper mainly consists of two methods: MMLS and NLPCA.

A. MMLS

A signal $x(n)$ is split into two data series, the approximation part $x_e(n)$ and the detail part $x_o(n)$, which correspond to the even and odd data series of $x(n)$,

respectively.

The detail signal $x_o(n)$ is predicted using information contained in $x_e(n)$ and is replaced by the prediction error

$$d(n) = x_o(n) - P(x_e(n)) \quad (3)$$

where the prediction operator P is defined as

$$P(x_e)(n) = \max \left\{ \frac{(N_0/8 - i) \times (x_e \circ g)(n)}{N_0/8} + \frac{i \times (x_e \bullet g)(n)}{N_0/8} \right\} \quad (4)$$

where $g = [0 \ 0.178 \ 0.356 \ 0.534 \ 0.712 \ 0.890 \ 0.712 \ 0.534 \ 0.356 \ 0.178 \ 0]$ is a triangular SE, $i = 1, 2, \dots, \lfloor N_0/8 \rfloor$, $i = \lfloor N_0/8 \rfloor$ means i takes the largest integer value that satisfies the equation $i \leq N_0/8$, and N_0 is the number of samples of a fundamental cycle.

The above scheme used to obtain $d(n)$ is the MMLS used in this paper, and $d(n)$, the output of the MMLS of signal $x(n)$, will be used to detect the existence of power disturbances. An example of a signal disturbed by voltage dip is shown in Fig. 3 (a), and the output of the MMLS of this signal is plotted in Fig. 3 (b). The impulse revealed in Fig. 3 (b), which corresponds to the position where this disturbance starts and is denoted by a , indicates the existence of power disturbances.

B. NLPCA

In Fig. 3 (a), c and d are two samples of $x(n)$ with the number of samples between c and a , and between a and d being $\lfloor N_0 \rfloor$ and $\lfloor N_0/2 \rfloor$, respectively. To determine the type of the power disturbance detected by the MMLS, the one-dimension signal between c and d is converted into a two-dimension signal $G(m) = (y(m), z(m))$, where $y(m) = x(m)$ and $z(m) = x(m - \lfloor N_0/4 \rfloor)$.

Afterwards, NLPCA is applied to extract the nonlinear principal components of $G(m)$ to determine the type of the power disturbance. As shown in Fig. 4, $G(m)$ and the nonlinear principal components of $G(m)$ are composed of the blue points and the red points, respectively.

In Fig. 4, the maximum and minimum distances between O , the center of the blue points, and the red points are expressed as r_{\max} and r_{\min} , respectively. Similarly, the maximum difference between two adjacent red points is expressed as l_{\max} . The three indices are used to classify power disturbances. In this case, $l_{\max} < 0.5$, $1 \leq r_{\max} < 1.1$ and $r_{\min} \leq 0.9$ are used to identify voltage dip.

SIMULATION STUDIES AND DISCUSSION

In this section, the proposed power disturbance scheme is applied to identify six types of power disturbances: voltage dip, voltage swell, momentary interruption, harmonics, notching, and transient oscillatory. PSCAD/EMTDC is employed to simulate these types of power disturbances. An example of the normalized signal used in this paper is shown in Fig. 1. As depicted in Fig. 1, six types of power disturbances appear in sequence in the signal. The flowchart of the proposed power disturbance identification scheme is shown in Fig. 2.

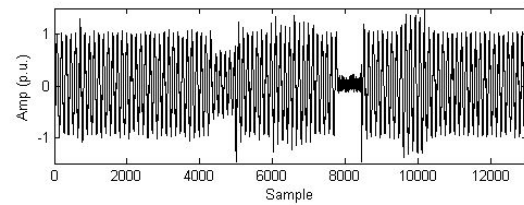


Fig. 1 The normalized signal used in this paper.

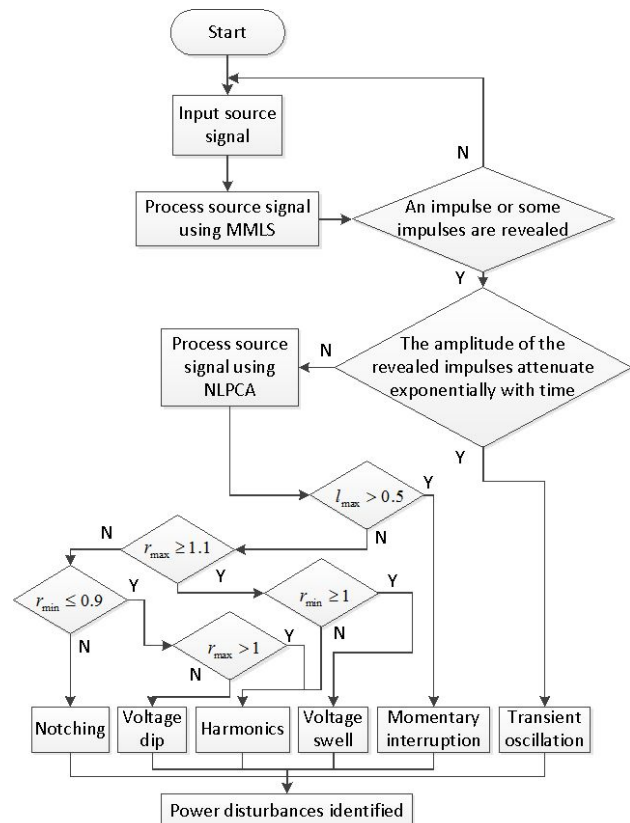


Fig. 2 The flowchart of the proposed power disturbance identification scheme.

A. Voltage dip

A case of the disturbance of voltage dip is shown in Fig. 3 (a). The output of the MMLS of this signal and the output of the NLPCA of $G(m)$ are depicted in Fig. 3 (b) and Fig. 4, respectively.

As discussed in the previous section, in this case, $l_{\max} < 0.5$, $1 \leq r_{\max} < 1.1$ and $r_{\min} \leq 0.9$ are used to identify voltage dip.

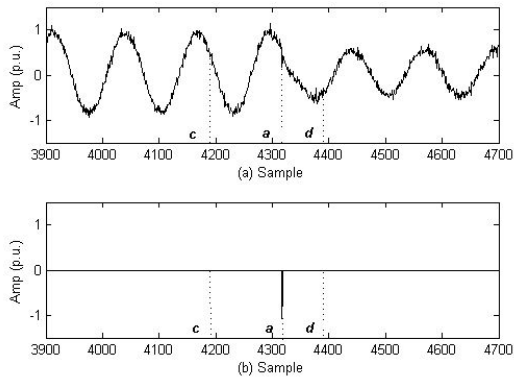


Fig. 3 (a) The disturbance of voltage dip; (b) the output of the MMLS of voltage dip shown in Fig. 3 (a).

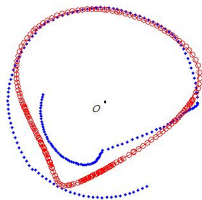


Fig. 4 $G(m)$ and the output of the NLPCA of $G(m)$ in the case of voltage dip detection.

B. Voltage swell

Figs. 5 (a) and (b) illustrate a power quality signal of voltage swell and the output of the MMLS of this signal, respectively. The output of the NLPCA of $G(m)$ in this case is described in Fig. 6. To detect voltage swell, $l_{\max} < 0.5$, $r_{\max} \geq 1.1$ and $r_{\min} \geq 1$ are applied.

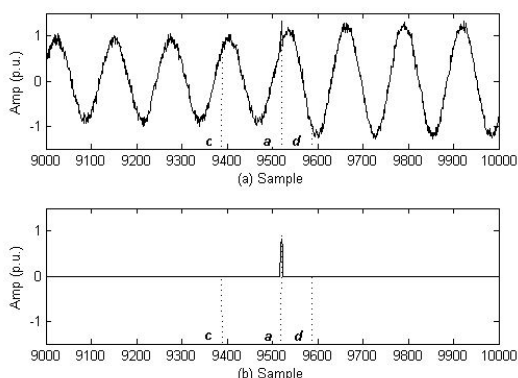


Fig. 5 (a) A power quality signal of voltage swell; (b) the output of the MMLS of voltage swell shown in Fig. 5 (a).

C. Momentary interruption

A simulation signal with momentary interruption and the output of the MMLS of this signal are described in Fig. 7.

In this example, the output of the NLPCA of $G(m)$ is depicted in Fig. 8. As shown in Fig. 8, the red points satisfy $l_{\max} \geq 0.5$, which is used to distinguish momentary interruption from other power disturbances.

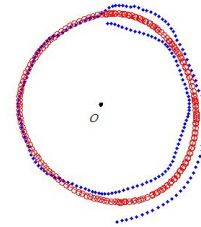


Fig. 6 $G(m)$ and the output of the NLPCA of $G(m)$ in the case of voltage swell detection.

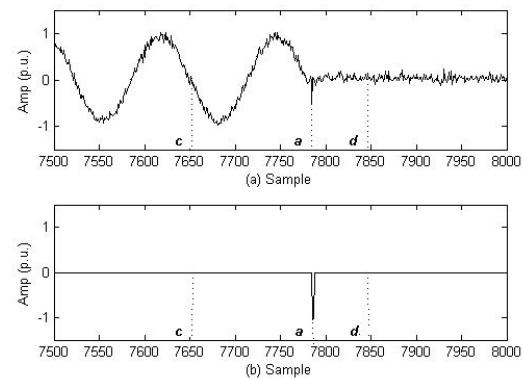


Fig. 7 (a) A simulation signal with momentary interruption; (b) the output of the MMLS of the signal shown in Fig. 7 (a).

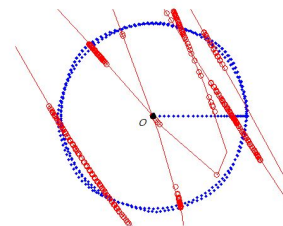


Fig. 8 $G(m)$ and the output of the NLPCA of $G(m)$ in the case of momentary interruption detection.

D. Harmonics

In Fig. 9, a power quality signal disturbed by harmonics and the output of the MMLS of this signal are presented, respectively. In Fig. 10, the output of the NLPCA of $G(m)$ in this example is depicted. A great deal of tests have been carried out by varying the components and amplitudes of harmonics, and the following two groups of indicators are observed for the identification of harmonics: $l_{\max} < 0.5$, $1 \leq r_{\max} < 1.1$, $r_{\min} < 0.9$ and $l_{\max} < 0.5$, $r_{\max} > 1.1$, $r_{\min} < 1$.

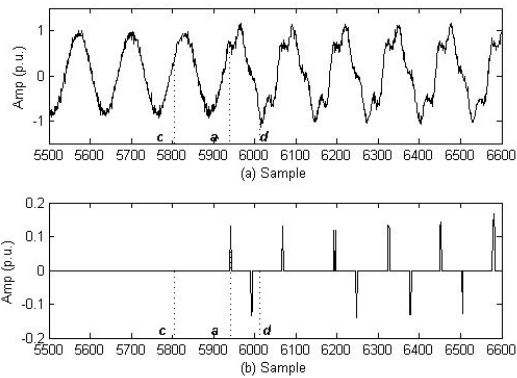


Fig. 9 (a) An power quality signal disturbed by harmonics; (b) the output of the MMLS of the signal shown in Fig. 9 (a).

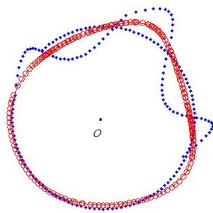


Fig. 10 $G(m)$ and the output of the NLPCA of $G(m)$ in the case of harmonics detection.

E. Notching

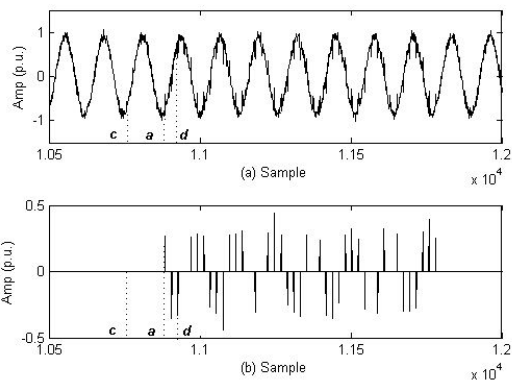


Fig. 11 (a) A fundamental sinusoidal signal affected by notching; (b) the output of the MMLS of the signal shown in Fig. 11 (a).

A fundamental sinusoidal signal affected by notching and the output of the MMLS of this signal are shown in Fig. 11. The output of the NLPCA of $G(m)$ in this case is depicted in Fig. 12. Based on trials and errors, $l_{\max} < 0.5$, $r_{\max} < 1.1$ and $r_{\min} > 0.9$ are used to identify notching.

F. Transient oscillation

Fig. 13 (a) describes a power quality signal disturbed by transient oscillation, and the output of the MMLS of this signal is plotted in Fig. 13 (b). In Fig. 13 (b), some

impulse are revealed, and the amplitudes of these impulses attenuate exponentially with time. Such a feature is used to identify transient oscillation.

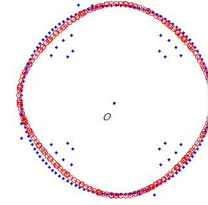


Fig. 12 $G(m)$ and the output of the NLPCA of $G(m)$ in the case of notching detection.

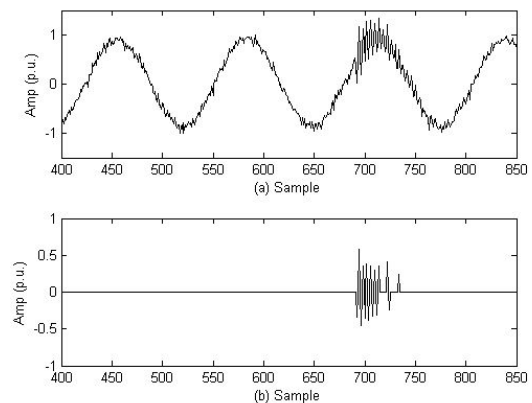


Fig. 13 (a) A power quality signal disturbed by transient oscillation; (b) the output of the MMLS of the signal shown in Fig. 13 (a).

CONCLUSION

A scheme based on transient behaviors using MMLS and NLPCA has been proposed in this paper to extract the features of various power disturbances. The scheme proposed in this paper can remarkably reduce the amount of calculation. PSCAD/EMTDC is used to simulate six types of power disturbances. The proposed scheme has been evaluated on massive test signals of these six types of disturbances. Simulation results have proved that the proposed scheme can identify these power disturbances quickly and accurately.

Acknowledgments

This project was supported by National Natural Science Foundation of China (No. 51207058) and Guangdong Innovative Research Team Program (No. 201001N0104744201).

REFERENCES

- [1] D. Granados-Lieberman, M. Valtierra, L. A. Morales-Hernandez, R. J. Romero-Troncoso, and R. A. Osornio-Rios, Jun 2014, "A hebert transform-based smart sensor for detection, classification, and

- quantification of power quality disturbance", *Sensors*, vol. 1, 5507-5527.
- [2] S. Juan, A. Noshadi, A. Kalam and S. Peng, Oct 2014, "Genetic algorithm optimised fuzzy control of DSTATCOM for improving power quality", *Power Engineering Conference (AUPEC), 2014 Australasian Universities*, vol. 1, 1-6.
- [3] C. I. Chen, Aug 2012, "Virtual multifunction power quality analyzer based on adaptive linear neural network", *Industrial Electronics, IEEE Transactions on*, vol. 59, no. 8, 3321-3329.
- [4] A. Dufour, T. Liu, C. Ducroz, R. Tournemene, B. Cummings, R. Thibeaux, N. Guillen, A. Hero, and J. Olivo-Marin, Dec. 2014, "Signal Processing Challenges in Quantitative 3-D Cell Morphology: More than meets the eye", *Signal Processing Magazine, IEEE*, vol. 32, no. 1, 30-40.
- [5] Q. H. Wu, Z. Lu, and T. Y. Ji, 2009, *Protective relaying of power systems using mathematical morphology*, Springer.
- [6] J. C. Diaz, N. Madrid, J. Medina, and M. Ojeda-Aciego, Jul. 2014, "New links between mathematical morphology and fuzzy property-oriented concept lattices", *2014 IEEE International Conference on Fuzzy Systems (FUZZ-IEEE)*, vol. 1, 599-603.
- [7] R. Radha and B. Lakshman, Mar. 2014, "Identification of Retinal Image Features Using Bitplane Separation and Mathematical Morphology", *2014 World Congress on Computing and Communication Technologies (WCCCT)*, vol. 1, 120-123.
- [8] S. T. Dogiwal, Y. S. Shishodia, and A. Upadhyaya, Sept. 2014, "Super Resolution Image Reconstruction using Wavelet Lifting Schemes and Gabor filters", *2014 5th International Conference on Confluence The Next Generation Information Technology Summit (Confluence)*, vol. 1, 625-630.
- [9] Y. Zhang, T. Y. Ji, M. S. Li, and Q. H. Wu, Dec. 2013, "Detection and classification of low-frequency power disturbance using a morphological max-lifting scheme", *Power and Energy Engineering Conference (APEEC)*, vol. 1, 1-5.
- [10] G. A. Licciardi, R. Dambreville, J. Chanussot, and S. Dubost, Aug. 2014, "Spatiotemporal Pattern Recognition and Nonlinear PCA for Global Horizontal Irradiance Forecasting", *Geoscience and Remote Sensing Letters, IEEE*, vol. 12, no. 2, 284-288.
- [11] Matthias Scholz, Martin Fraunholz, and Joachim Selbig, 2008, *Principal Manifolds for Data Visualization and Dimension Reduction*, Springer Berlin Heidelberg, New York, U.S.A., 44-67.
- [12] Matthias Scholz, Fatma Kalan, Charles L. Gug, Jiachim Kopka, and Joachim Selbig, Aug. 2005, "Non-linear PCA: a missing data approach", *Bioinformatics*, vol. 21, no. 20, 3887-3895.